# Rotational Motion of a Free Body Induced by Mass Redistribution

John E. Cochran Jr.* and Norman O. Speakman†
*Auburn University, Auburn, Ala.*

**The effects of mass redistribution on the rotational motion of a free body, initially rotating uniformly about its axis of maximum moment of inertia, are studied using a simple three-body model composed of two "control" points masses and a triaxial rigid body. An exact analytical solution for the motion of the original spin axis after redistribution of the masses is developed from the classical solution for the rotational motion of a free triaxial rigid body. Yhis motion in interpreted geometrically using the reciprocal inertia ellipsoid of the redistributed system and the angular momentum integral. Application of simple mass redistribution to the problem of spacecraft attitude control is discussed and results for a particular system are presented.**

## Introduction

IT is a well-known fact[1] that for a free, triaxial, rigid body, the condition of uniform rotation about its axis of intermediate, principal moment of inertia is unstable. This instability manifests itself when small disturbances in the angular velocity components about the other principal axes occur; for then, the once-stationary axis of intermediate moment of inertia performs large-angle motions with respect to a nonrotating reference frame. Recently, Beachley and Uicker[2] and Beachley,[3] have suggested that this characteristic of rigid body rotational motion might be used to advantage to "control" a spinning spacecraft in the sense that predictable large-angle motions of an axis fixed in the spacecraft might be induced by changing the mass distribution of the spacecraft.‡ A control system based on this idea might be more economical than a mass expulsion system which would rotate the angular momentum vector of the spacecraft.

Changes in the mass distribution of the spacecraft may be accomplished by internal motion of control masses. The effects of such internal mass motion on the rotational motion of a free system of bodies have been studied by several authors and a review of some of the work in this area is given by Lorell and Lange,[5] who propose an automatic mass-trim system for spinning spacecraft which utilizes movable control masses.

The primary purpose of this paper is not to study the effects of internal mass motion on the rotational motion of a free system of bodies, although these effects cannot be ignored entirely and will be considered. Our main goal is to obtain an analytical description of the spacecraft's rotational motion after a redistribution of mass has occurred. Such a description has previously been obtained only in a limited way by numerical integration.[3] We shall also provide geometrical interpretation of the analytical results and consider the use of simple mass redistribution as a means for spacecraft attitude control. In this paper we shall consider a system similar to those discussed in Ref. 3 and employ some results from the classical theory for the rotational motion of a free, triaxial, rigid body.

Received June 12, 1974; revision received November 1, 1974.
Index category: Space Attitude Dynamics and Control.

*Assistant Professor, Aerospace Engineering. Member AIAA.

†Formerly, Graduate Student, Aerospace Engineering; presently, Second Lieutenant, USAF, Eglin, AFB, Fla.

‡Actually, Kane and Scher[4] earlier suggested a very similar method for active spacecraft attitude control.

## Spacecraft Model

The system we shall consider is shown in Fig. 1. It consists of a single rigid body, with center of mass $C$, and two point-mass control masses, each of mass $m$. We assume that no external moments act on the system and that the control masses are constrained to move in the $yz$-plane of the $Cxyz$ coordinate system, which is a principal system for the rigid body. It is also assumed that the control masses may be moved in any manner in the $yz$-plane, as long as the center of mass of the system always coincides with $C$.

The principal moments of inertia of the rigid body are denoted by $I_x$, $I_y$, and $I_z$, and, in the initial steady-spin configuration of the composite body, the control masses are located on the $\pm$ $y$-axes, each a distance $\mathcal{L}$, from $C$ and the composite body is rotating about the $z$-axis. The moments of inertia of the rigid body, the mass $m$, and distance $\mathcal{L}$, are required to be such that $I_z + 2m\mathcal{L}^2 > I_y > I_z > I_x$. Hence, if, for example, the control masses are moved sufficiently close to the $z$-axis, that axis will no longer be the axis of maximum moment of inertia and the system's state will depart from that corresponding to the initial steady-spin condition. Various types of departures from the initial steady state can be achieved by different types of mass movement.

If the control masses are moved in along the $\pm$ $y$-axes, the forces required to move (and constrain) them with respect to the rigid body act in the $xy$-plane and produce a torque on the rigid body about its $z$-axis only. In this case, the only change in the steady-spin condition will be an increase in the composite body's spin rate so that the angular momentum of the system remains constant as the spin-axis moment of inertia decreases.

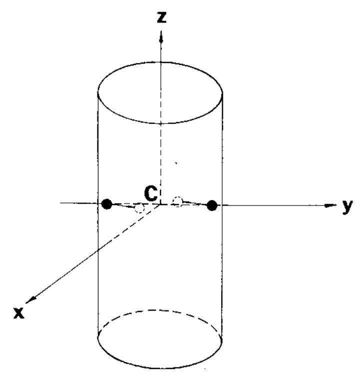


Fig. 1 System model.

Motion of the control masses off the $y$ axis will result in a more general reaction torque on the rigid body and the $x$ and $y$ components of the angular velocity of the $Cxyz$ system will not remain zero, although they may remain small. Furthermore, the principal axes of the system will, in general, change when the control masses are moved and the constant angular momentum vector of the system will not remain colinear with a principal axis. Thus, the composite body will, in general, begin to rotate in a "nonuniform" manner. Depending on the final positions of the control masses and the manner in which they are moved, motions corresponding to the various rotational states of a free, triaxial, rigid body will result. Portions of some of these motions correspond to almost exact inversions of the composite body.

## Rotational Motion after Mass Redistribution

We depart from the natural order of occurrence of events by first considering the rotational motion of the composite body after the internal mass redistribution has ceased at time $t_l$ and the system can again be considered to be a single rigid body. The rotational motion of the system during the time of control mass motion, $t_0 \leq t < t_{l0}$, will be considered later.

When the control masses are in positions, $(0, y_l, z_l)$ and $(0, y_l, -z_l)$, respectively, at $t = t_l$, the new principal axes of the composite body are $x'$, $y'$, and $z'$, as shown in Fig. 2. These axes are rotated with respect to the original principal axes through an angle $\chi$ so that

$$\begin{pmatrix} x' \\ y' \\ z' \end{pmatrix} = \begin{bmatrix} 1 & 0 & 0 \\ 0 & c\chi & s\chi \\ 0 & -s\chi & c\chi \end{bmatrix} \begin{pmatrix} x \\ y \\ z \end{pmatrix} \tag{1}$$

where $\chi = \frac{1}{2}\tan^{-1}\{my_l z_l / [I_z - I_y + 2m(y_l^2 - z_l^2)]\}$.§ The $x'$, $y'$, and $z'$ angular velocity components, $\omega_{x'}$, $\omega_{y'}$, and $\omega_{z'}$, are also related to $\omega_x$, $\omega_y$, and $\omega_z$, through the transformation matrix appearing in Eq. (1).

If we use the modified Eulerian angles, $\psi$, $\theta$ and $\phi$, depicted in Fig. 3, the orientation of the $Cx'y'z'$ coordinate system with respect to a nonrotating $Cx_h y_h z_h$ coordinates system, which has its $z_h$-axis colinear with the rotational angular momentum vector $\mathbf{h}$ of the system, may be defined. Explicitly, we have

$$\begin{pmatrix} x' \\ y' \\ z' \end{pmatrix} = \begin{bmatrix} 1 & 0 & 0 \\ 0 & c\phi & s\phi \\ 0 & -s\phi & c\phi \end{bmatrix} \begin{bmatrix} c\theta & 0 & -s\theta \\ 0 & 1 & 0 \\ s\theta & 0 & c\theta \end{bmatrix} \begin{bmatrix} c\psi & s\psi & 0 \\ -s\psi & c\psi & 0 \\ 0 & 0 & 1 \end{bmatrix} \begin{pmatrix} x_h \\ y_h \\ z_h \end{pmatrix} \tag{2}$$

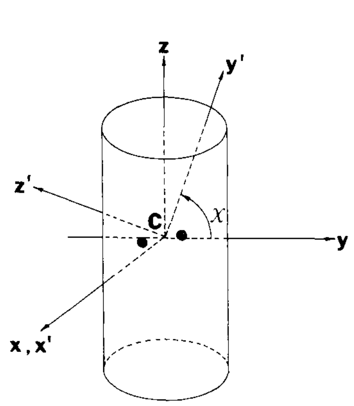


Fig. 2 System configuration and principal axes after mass motion.

§The notation, $c \equiv$ cosine and $s \equiv$ sine, is used where conciseness is desirable.

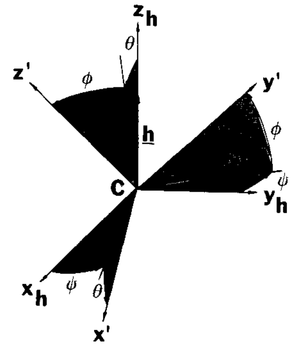


Fig. 3 Eulerian angles.

After the internal motion of the control masses ceases, the composite body is rigid and we may use the classical solution[6] for free-Eulerian motion in which the Eulerian angles, $\psi$, $\theta$ and $\phi$, are expressed analytically as functions of time using Jacobian elliptic functions and Theta functions.¶

A brief derivation of the solution is presented in the Appendix of this paper for completeness. The results which we need at present are

$$\begin{aligned} \sin\theta &= -p\, cn\, u \\ \cos\theta \sin\phi &= q\, sn\, u \\ \cos\theta\cos\phi &= r\, dn\, u \end{aligned} \tag{3}$$

and

$$\psi = \psi_l + (n/\Omega)(\tau - \tau_l) - \frac{i}{2}\ln\left[\frac{\Theta(u - ia')\Theta(v - ia')}{\Theta(u + ia')\Theta(v + ia')}\right] \tag{4}$$

In Eqs. (3) and (4), $u = \lambda(t - t_l) - v$ and constants $p$, $q$, $r$, $n$, $\lambda$, $v$, and $a'$, are defined in the Appendix.** Also, $\tau = t\Omega$, where $\Omega$ is the spacecraft's spin rate before the control masses are moved, $\psi_l$ is the value of $\psi$ when $t = t_l = \tau_l/\Omega$ and $i = \sqrt{-1}$. Furthermore, in Eqs. (3), $cn\, u$, $sn\, u$, and $dn\, u$ are Jacobian elliptic functions of modulus $k$ (see Appendix) and in Eq. (4), $\Theta(\ )$ is Jacobi's theta function.

If one is only concerned with the angle $\gamma$ between the angular momentum vector $\mathbf{h}$ and the original spin axis $z$ (see Fig. 4) then the precession angle $\psi$ is not needed; for, from the geometry of Fig. 4, we have

$$\cos\gamma = \sin\chi\cos\theta\sin\phi + \cos\chi\cos\theta\cos\phi \tag{5}$$

Now, at time, $t_l$,

$$\begin{bmatrix} \omega_{x'} \\ \omega_{y'} \\ \omega_{z'} \end{bmatrix} = h \begin{bmatrix} p\ cn\ v \\ -q\ sn\ v \\ r\ dn\ v \end{bmatrix} = \begin{bmatrix} 1 & 0 & 0 \\ 0 & cx & sx \\ 0 & -sx & cx \end{bmatrix} \begin{bmatrix} \omega_x \\ \omega_y \\ \omega_z \end{bmatrix} \tag{6}$$

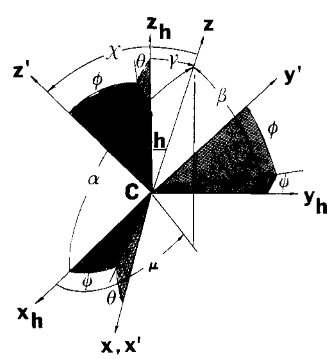


Fig. 4 Eulerian angles and orientation of the $z$-axis.

¶Eulerian angles which are different from those in Ref. 6 are adopted here, and the form of the solution is therefore slightly different. See also Ref. 1, pp. 196-198.

**A reader not familiar with the solution to the problem of free rotational motion of a *triaxial* rigid body is advised to consult the Appendix at this point.

where $h$ is the magnitude of the angular momentum, and by letting $A$, $B$ and $C(C>B>A)$ denote the principal moments of inertia of the composite body at time $t_1$ we have, from Eqs. (3) and (6),

$$\begin{aligned} -\sin\theta_1 &= A\omega_{x_1}/h \\ \cos\theta_1 \sin\phi_1 &= B/h[\omega_{y_1}\cos\chi+\omega_{z_1}\sin\chi] \\ \cos\theta_1 \cos\phi_1 &= C/h[-\omega_{y_1}\sin\chi+\omega_{z_1}\cos\chi] \end{aligned} \tag{7}$$

where the subscript 1 denotes the value of the subscripted variable at time $t_1$. The value of $\cos\gamma$ at the end of the mass redistribution is therefore

$$\cos\gamma_1 = [(B-C)/2h]\omega_{y_1} s2\chi + [(Cc^2\chi+Bs^2\chi)/h]\omega_{z_1} \tag{8}$$

or

$$\cos\gamma_1 = 2my_1z_1\omega_{y_1}/h + (I_z+2my_1{}^2)\omega_{z_1}/h \tag{9}$$

The maximum angle between **h** and the $z$-axis, $\gamma_\omega$, determined from the expression,

$$\cos\gamma = q\sin\chi\, sn\, u + r\cos\chi\, dn\, u \tag{10}$$

is

$$\gamma_m = \cos^{-1}[-q\sin\chi + r(1-k^2)^{1/2}\cos\chi] \tag{11}$$

and occurs when $\omega_{x'}=0$; e.g., when $u=3K$, where $K$ is the complete elliptic integral of the first kind of modulus, $k$.

The constant of integration, $\nu$, and the constants $q$ and $r$ deserve some special consideration at this point so that some interesting results may be obtained. If $\omega_{x_1}$ and $\omega_{y_1}$ are much less than $\omega_{z_1}$, then from Eqs. (6), $\nu \simeq -Kq \simeq (B\omega_{z_1}/h)\sin\chi$, and $r(1-k^2)^{1/2} \simeq (C\omega_{z_1}/h)\cos\chi$.†† These assumptions as to the size of $\omega_{x_1}$ and $\omega_{y_1}$ allow us to obtain the approximations, $h/\omega_{z_1} \simeq I_z + 2my_1{}^2 \equiv I_{z_1}$ and

$$\gamma_m \simeq \cos^{-1}\left[\frac{B-C}{2I_{z_1}} + \frac{B+C}{2I_{z_1}}\cos 2\chi\right] \tag{12}$$

Then, using well known formulas for principal moments of inertia, we get

$$\gamma_m \simeq \cos^{-1}\left[\cos 2\chi + \frac{2my_1z_1}{I_{z_1}}\sin 2\chi\right] \tag{13}$$

Finally, by defining $\delta \equiv 2my_1z_1/I_{z_1}$ and assuming $|\delta| \ll 1$, we may rewrite Eq. (13) as

$$\gamma_m \simeq 2\chi - \delta \tag{14}$$

For $\delta \geq 0$, $\chi$ is at most $\pi/2$, and to achieve $\gamma_m \simeq \pi$ (an almost exact inversion), $\delta$ should be made as small as possible. Also, since $\tan 2\chi = 2\delta/(I_{z_1}-I_{y_1})$, where $I_{y_1}=I_y+2mz_1{}^2$, $I_{y1}$ should be greater than $I_{z1}$, but $I_{y_1}/I_{z_1}$ should be made as near unity as feasible. The above analytical result [Eq. (14)] supports the conclusions obtained in Ref. 3 on the basis of numerical studies.

Equations (10) and (11) may be interpreted geometrically. The apparent movement of the "invariable axis" (axis colinear with **h** in the reciprocal ellipsoid, $x'^2/A+y'^2/B+z'^2/C=1$, where $x'=-\rho s\theta$, $y'=\rho c\theta s\phi$, $z'=\rho c\theta c\phi, \rho^2=h^2/2T$ and $T$=rotational kinetic energy, may be displayed graphically as in Fig. 5. When the characteristics of the rigid body and control masses are known, $\chi$ is specified and the ratio, $\rho$, has been determined, the intersection of the sphere, $x'^2+y'^2+z'^2=\rho^2$, with the reciprocal ellipsoid, in general, consists of two curves on the ellipsoid. One of these is traced out by the invariable axis as time passes. For example, the point at which the invariable axis pierces the ellipsoid might be represented by $A'$ at $t=t_1$. Then, clearly, the maximum angle between **h** and the $z$—axis occurs when the pierce point is $B'$. At $B'$, $\mathbf{h}_{x'}=0$, so that if $\omega_x \simeq 0$ at $t=t_1$, the time to achieve $\gamma_m$ is approximately $2K/\Lambda$.

For a complete inversion ($\gamma_m=180°$), the points, $A'$ and $B'$, must lie on the $y'$-axis as shown in Fig. 5b. As this "ideal" case is approached, the periods of the elliptic functions ($4K/\lambda$ for $sn\, u$ and $cn\, u$ and $2K/\lambda$ for $dn\, u$) approach infinity and the motion is not of practical interest. However, values of $\gamma_m$ very close to 180° may be achieved while retaining reasonable values for $2K/\lambda$, since $K<6$ for $k<0.99985$.[7] The steepness of the $K$ vs $k$ curve near $k=1$ has other ramifications which will be discussed later.

Obviously, if the control masses are not moved a second time the angle, $\gamma$, will ultimately return to its value at $t=t_1$. If, however, $\gamma_m \simeq \pi$ and the control are returned to their original positions while $\gamma \simeq \gamma_m$, the result is that the spacecraft's *negative* $z$-axis will remain "almost" aligned with the angular momentum vector. The small angle between **h** and the $-z$-axis might then be forced to zero by releasing the damper mass (heretofore constrained) of a damper mechanism or by other means.

Since the Jacobian elliptic functions may be computed using readily available computer subroutines,‡‡ the solution [Eq. (10)] for $\cos\gamma$ may be used instead of numerical integration to study the inversion problem with considerable savings in computer time. In fact, if only the maximum turning angle and time required for the inversion are desired, one need only integrate the equations of motion for the changing system, find $\omega_{x_1}$, $\omega_{y_1}$, $\omega_{z_1}$, $\chi$, $A$, $B$, and $C$ and then compute $q$, $r$, $\lambda$, $k$, and $K$. The complete elliptic integral $K$ may be obtained using a computer subroutine or from tables such as those in Ref. 7. Furthermore, if all the dynamic effects of moving the control masses, except the change in $\omega_z$, are ignored, the following formulas for $k$ and $\lambda$ may be used to compute $K$ and the time to reach $\gamma_m \simeq 2\chi$:

$$k \simeq 1 - c^2\chi\left[\frac{(C-A)[C-(C-B)s^2\chi]}{C[(C-A)-(C-B)s^2\chi]}\right]^{1/2} \tag{15}$$

$$\lambda \simeq h/c[(C-B)(A-C)/AB]^{1/2} \times \left[-\frac{C[(C-A)-(C-B)s^2\chi]}{(C-A)[C-(C-B)s^2\chi]}\right] \tag{16}$$

Note that if $(C-B)/(C-A) \ll 1$, $k \simeq \sin\chi$ and $\lambda \simeq (h/C)[(C-B)(C-A)/AB]^{1/2}$. This is the case when $|I_{z_1}-I_{y_1}|/|I_z-I_{x_1}| \ll 1$ and $|2\delta|/|I_{z_1}-I_{x_1}| \ll 1$. Finally, approximate analytical solutions for the transient motion such as the one discussed in the next section may be used to circumvent numerical integration entirely, while not ignoring the transient motion effects on the "steady-state" tumbling motion.

An inversion may not be the maneuver required for a spacecraft. Suppose, for example, that a spacecraft contains a sensor of some type with a limited field of view which is oriented in the $+z$-direction. Also, suppose that the control masses are moved so that an angle $\chi$ between 0 and $\pi/8$ will result from their final displacements.§§ As $\gamma$ increases and then decreases, the $z$-axis will move on the surface of a cone with axis parallel to **h**, vertex at $C$ and semivertex angle $\gamma$. The projection $P$ of the terminus of a unit vector $\hat{\mathbf{k}}$, directed along the $z$-axis from $C$, onto the $x_hy_h$-plane will follow a spiral path out from a distance of $\sin\gamma_1$ at $t_1$ to a maximum distance, $\sin\gamma_m$, at $T-T_1 \simeq 2K/\lambda$ and then return to a distance, sin

††Information contained in the Appendix is needed to obtain these approximations for $q$ and $r$.

‡‡For example, the IBM Scientific Subroutine Package contains subroutines for computing these functions.

§§If $\pi/8<\chi<3\pi/8$, the previous results must be modified by replacing $\chi$ with $\chi-\pi/2$.

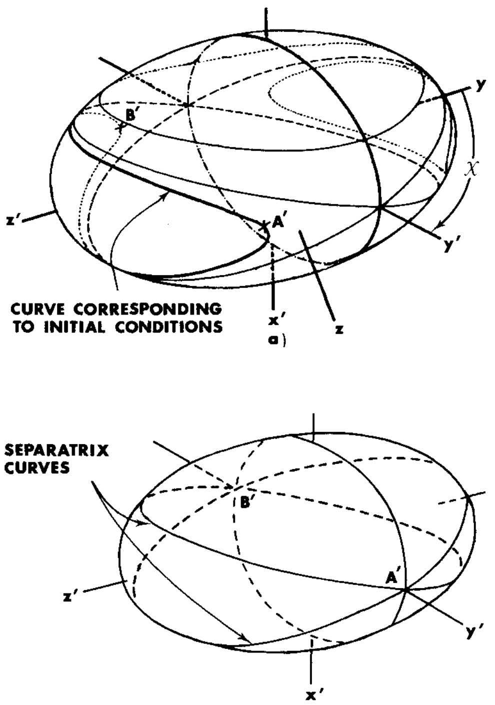


**Fig. 5 Geometric representation of the spin axis motion.**

$\gamma_1$, from the origin at $t-t_1=4K/\lambda$. The position of $P$ in the $x_h y_h$ – plane will not usually be the same at times, $t_1$ and $t_1+4K/\lambda$, since the periods of precession and nutation are not in general commensurable. However, if the spacecraft's period of precession is much smaller than $4K/\lambda$, the loci of the point $P$ will essentially cover a circle of radius sin $\gamma_m$, with center $C$, and the sensor will "scan" an area of the celestial sphere determined by the maximum cone angle $\gamma_m$. By returning the control masses to their original positions when $\gamma=\gamma_1$ the second time and removing the residual nutation angle with dampers, the spacecraft could be returned essentially to its initial steady-state.

To obtain the complete motion of the $z$-axis, we introduce angle $\mu$ shown in Fig. 4. Then from geometry, we have

$$\tan\mu=\cos\beta/\cos\alpha \tag{17}$$

where

$$\begin{aligned}\cos\alpha &= \sin\chi[-\cos\phi\ \sin\psi+\sin\theta\ \cos\psi]\\ &\quad+\cos\chi[-\sin\phi\ \sin\psi+\sin\theta\ \cos\phi\ \cos\psi]\\ \cos\beta &= \sin\chi[\cos\phi\ \cos\psi+\sin\theta\ \sin\phi\ \sin\psi]\\ &\quad+\cos\chi[-\sin\phi\ \cos\psi+\sin\theta\ \cos\phi\ \sin\psi]\end{aligned}$$

When $\chi$ is small $\mu\simeq\psi$.

The time variation of $\psi$ may be obtained from Eq. (4). This was not done, however, to obtain the results which we present later. Instead, the variable term $[h(C-B)/BC]\ \sin^2\phi$, of $\dot\psi$ was integrated numerically and added to the "dominant" (for the examples treated here) part, $(h/C)(t-t_1)+\psi_1$, of $\psi$.

To determine $\mu$, we also need the expressions,

$$\theta=\sin^{-1}(-p\ cn\ u) \tag{18}$$

and

$$\phi=\tan^{-1}(q\ sn\ u/r\ dn\ u) \tag{19}$$

which follow from Eqs. (3).

## Rotational Motion During Mass Movement

The initial conditions needed in the analytical solutions previously derived must, in general, be obtained by numerically integrating the differential equations which govern the rotational motion of the system while the control masses are moving. The necessary equations for $\omega_x$, $\omega_y$, and $\omega_z$ may be obtained from

$$\mathrm{d}\boldsymbol{h}/\mathrm{d}t=\delta\boldsymbol{h}/\delta t+\boldsymbol{\omega}\times\boldsymbol{h}=0 \tag{20}$$

where

$$\begin{aligned}\boldsymbol{h}=&\{[I_x+2m(y^2+z^2)]\omega_x-2m(\dot yz-y\dot z)\}\,\hat{\imath}\\ &+\{(I_y+2mz^2)\omega_y-2myz\omega_z\}\hat{\jmath}\\ &+\{(I_z+2my^2)\omega_z-2myz\omega_y\}\hat{k}\end{aligned} \tag{21}$$

$\delta/\delta t$ indicates that only the time derivatives of the components of $\boldsymbol{h}$ are to be taken and $\hat{\imath}$, $\hat{\jmath}$, and $\hat{k}$ are unit vectors associated with the $Cxyz$ system.

Dimensionless scalar equations may be obtained from Eqs. (20) and (21) by introducing the notation,

$$\sigma_1=I_x/I_z;\ \sigma_2=I_y/I_z;\ \sigma_3=2m\mathcal{L}^2=I_z$$

$$\eta=y/\mathcal{L};\zeta=z/\mathcal{L};\ \lambda_x=\omega_x/\Omega;$$

$$\lambda_y=\omega_y/\Omega;\lambda_z=\omega_z/\Omega;d(\ )/d\tau=(\ )'$$

The dimensionless equations for the angular velocity components are

$$\begin{aligned}\lambda'_x=&\{-2\lambda_x\sigma_3(\zeta\zeta'-\eta\eta')+(\sigma_2-1)\lambda_y\lambda_z+\\ &\sigma_3[(\zeta^2-\eta^2)\lambda_y\lambda_z+(\lambda_y{}^2-\lambda_z{}^2)\eta\zeta]+\\ &\sigma_3(\zeta\eta''-\eta\zeta'')\}/[\sigma_1+\sigma_3(\eta^2+\zeta^2)]\\ \lambda'_y=&[(1+\sigma_3\eta^2)D+\sigma_3\eta\zeta E]/[\sigma_2+\sigma_3(\zeta^2+\eta^2\sigma_2)]\\ \lambda'_z=&[(\sigma_2+\sigma_3\zeta^2)E+\sigma_3\eta\zeta D]/[\sigma_2+\sigma_3(\zeta^2+\eta^2\sigma_2)]\end{aligned} \tag{22}$$

where

$$\begin{aligned}D=&2\sigma_3\zeta(\lambda_z\eta'-\lambda_y\zeta')+(1-\sigma_1\\ &-\sigma_3\zeta^2)\lambda_x\lambda_z-\sigma_3\eta\zeta\lambda_x\lambda_y\\ E=&2\sigma_3\eta(\lambda_y\zeta'-\lambda_z\eta')+(\sigma_1\\ &-\sigma_2+\sigma_3\eta^2)\lambda_x\lambda_y+\sigma_3\eta\zeta\lambda_x\lambda_z\end{aligned}$$

Equations (22) agree with analogous equations given in Ref. 3 except for a sign difference which is due to the use of a left-handed coordinate system in that study.

A dimensionless differential equation for $\psi$ may also be obtained. From geometrical considerations, we have, using $\psi$, $\theta_T$ and $\theta_1$ as the Eulerian angles in a 3-2-1 rotational sequence,

$$\psi'=(\lambda_x\sin\theta_1+\lambda_y\cos\theta_1)/\cos\theta_2 \tag{23}$$

where

$$\theta_1=\tan^{-1}\left[\frac{(\sigma_2+\sigma_3\zeta^2)\lambda_y-\sigma_3\eta\zeta\lambda_z}{(1+\sigma_3\eta^2)\lambda_z-\sigma_3\eta\zeta\lambda_y}\right]$$

and

$$\theta_2=-\sin^{-1}\left[\frac{[\sigma_1+\sigma_3(\eta^2+\zeta^2)]\lambda_x-\sigma_3[\zeta\eta'-\eta\zeta']}{(1+\sigma_3)}\right]$$

Fairly accurate estimates of the dynamical effects of the control mass motion may be obtained from Eqs. (22) in closed form under certain conditions. For example, if the control masses are moved in along the $\pm y$-axes during time, $t_0 < t \leq t^* < t_1$, to the desired $y$-coordinates and then moved parallel to the $z$-axis during time, $t^* < t \leq t_1$, to their final positions, Eqs. (22) are greatly simplified.

During the motion of the control masses along the $\pm y$-axes, the solution to Eqs. (22) is

$$\begin{aligned} \lambda_x &= 0 \\ \lambda_y &= 0 \\ \lambda_z &= (1+\sigma_3 \eta_0^2)/(1+\sigma_3 \eta^2), t_0 < t < t^* \end{aligned} \tag{24}$$

regardless of how the motion occurs in time. Then, assuming that $1-\sigma_2$, $\sigma_3$, $|\lambda_x|$, and $|\lambda_y|$ are small during the motion of the masses parallel to the $z$-axis, Eqs. (22) may be approximated during the second time interval by

$$\lambda'_x \simeq -\sigma_3/\sigma_1(\eta_1 \zeta'' - \lambda^2_{z_1}\eta_1 \zeta) \tag{25}$$

$$\lambda'_y \simeq [(1-\sigma_1)/\sigma_2]\lambda_{z_1}\lambda_x \tag{26}$$

and

$$\lambda_z \simeq \lambda_{z_1} = (1+\sigma_3 \eta_0^2)/(1+\sigma_3 \eta_1^2), \ t^* < t \leq t_1 \tag{27}$$

If we judiciously choose a time variation from $\zeta$, Eq. (25) may be easily integrated by quadratures. For example, if $t_0 = 0$, $t^* = t_1/2$ and

$$\zeta = \tfrac{1}{2}\zeta_1\{1-\cos[2\pi(\tau-\tau_1/2)/\tau_1]\}, \ \tau_1/2 < \tau < \tau_1 \tag{28}$$

then

$$\lambda_{x_1} \simeq -(\sigma_3/\sigma_1)\eta_1 \zeta_1 \lambda^2_{z_1}\tau_1/2 \tag{29}$$

Also, we obtain for $\lambda_{y_1}$ the solution,

$$\begin{aligned} \lambda_{y_1} \simeq -[\sigma_3(1-\sigma_1)/\sigma_1\sigma_2]\lambda_{z_1}[\eta_1\zeta_1 \\ + \lambda^2_{z_1}\eta_1 \zeta \tau_1^2((\pi^2-4)/16\pi^2)] \end{aligned} \tag{30}$$

Approximate values for $\lambda_{x_1}$ and $\lambda_{y_1}$ were computed for several examples using the system parameters given in the next section and Eqs. (29) and (30) and initial values of $\gamma$ within 5% of those obtained by numerical integration were calculated.

## Results

To verify the analytical results for $\cos\gamma$, the specific values for system parameters given in Table 1 were adopted. In addition to the motion of the masses specified by Eq. (28), straight-line paths for the control masses were chosen and the following forms for the coordinates of the control masses as functions of time were assumed:

$$y = y_0 + (y_0 - y_1)[2(t/t_1)^3 - 3(t/t_1)^2]$$

$$z = b(y - y_0)$$

The initial $y-$ and $z-$coordinates are given also in Table 1. The final $y-$ and $z-$coordinates were determined by the requirements that $[(I_z + 2my_1^2)/(I_y + 2mz_1^2)]$ and $\chi$ have specified values.

**Table 1 System parameters**

| | |
|---|---|
| Initial spin rate (rpm) | 100.0 |
| Moments of inertia of main body: $I_x$, $I_y$, $I_z$ (slug-ft$^2$) | 72.75, 76.90,7622 |
| Mass of each control mass (slugs) | 0.075 |
| Initial mass position: $y_0$, $z_0$ (ft) | 5.0, 0.0 |

Equations (22) and (23) were integrated numerically to obtain the initial conditions for various values of $\chi$. The angle $\gamma$-was determined using Eq. (10) and checked out by continuing the numerical integration of Eqs. (22) after the control masses had stopped moving, using the fact that $\cos\gamma$ is also given by

$$\cos\gamma = \frac{[(1+\sigma_3\eta_1^2)\lambda_z - \sigma_3\eta_1\zeta_1\lambda_y]}{[h/(I_z\Omega)]} \tag{31}$$

The results for $\gamma$ agreed within the limits of numerical precision.

Figure 6 shows some of the time histories for $\gamma$ which were obtained using a mass motion time period of 0.1 sec. For such rapid motion of the control masses, $\lambda_x$ and $\lambda_y$ remain very small $[(10^{-3})]$ and $\gamma_m$ is almost exactly $2\chi$. The increase in turnover time for smaller values of $\chi$ is due to smaller values of $\lambda$, since the values of $K$ are actually smaller.

Figure 7 shows the effect of increasing the time required to move the masses. In Fig. 7, the value of $\chi$ for each curve is 86° and the control mass motion times used were 0.1, 1, and 10 sec. The results indicate that the time required to move the mass does not have a significant effect on the motion of the system, if it is small compared to $2K/\lambda$.

"Coning maneuvers" of a spacecraft with the characteristics given in Table 1 may be caused by specifying $\chi \leq \pi/8$ and $I_{z_1}/I_{y_1} < 1$. The results for $\gamma$ shown in Fig. 8 were obtained using $I_{z_1}/I_{y_1} = 1.01$ and a mass motion time of one sec. For angles $\chi$ indicated, the time variation in $\mu$ was so rapid that $\lambda$ did not change by a discernible amount while $\mu$ changed by $2\pi$; i.e., the sections of the celestial sphere intersected by the cones with vertex angles equal to the respective values of $2\gamma_m$ would be covered almost completely by a sensor on the-$z$-axis of such a spacecraft.

Another choice of spin rate, $\Omega = 1$ rpm, was used along with $I_{z_1}/I_{y_1} = 0.99$ and $\chi = 80°$ to obtain Fig. 9, which shows $x_h = \sin\gamma\cos\mu$ and $y_h = \sin\gamma\sin\mu$ for a period of time when $\gamma$ was near 80°.

## Possible Applications

As pointed out in Ref. 3, it may be desirable to invert a spinning spacecraft to protect certain devices from solar radiation. The theory presented here should be useful in designing a system to accomplish this.

As we have also shown, a possible application for mass redistribution control would be that of producing a variable "coning" $\gamma$ to allow an instrument on the original spin axis of

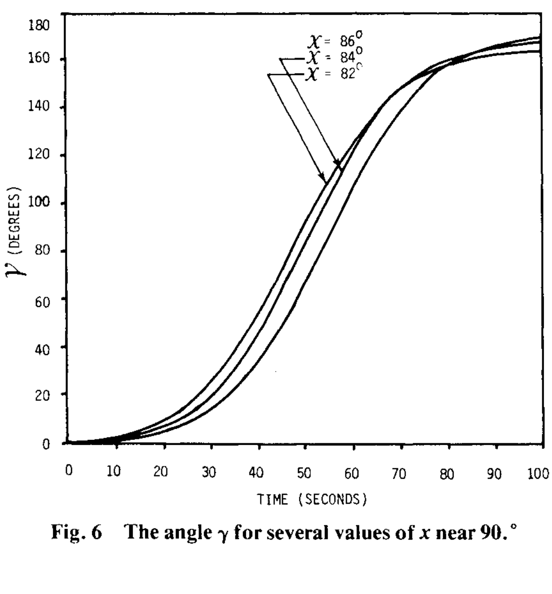


**Fig. 6 The angle $\gamma$ for several values of $x$ near 90.°**

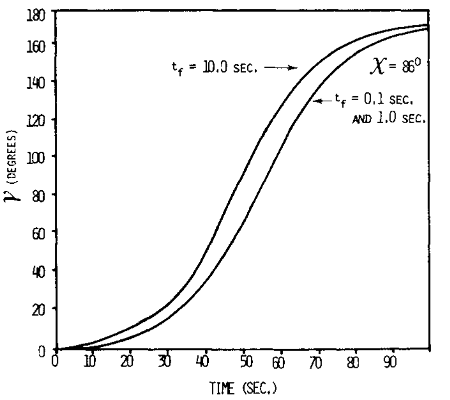


**Fig. 7 Effect of mass transit time on $\gamma$.**

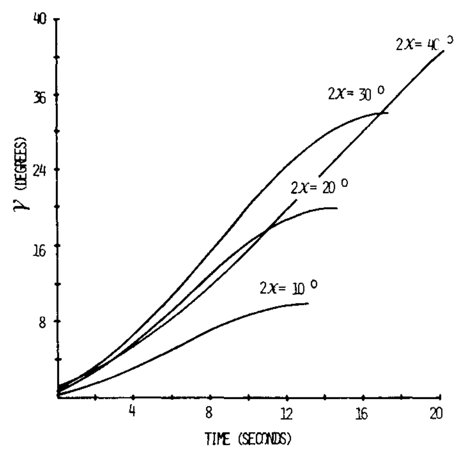


**Fig. 8 Cone semivertex angles for $2x<\pi/4$.**

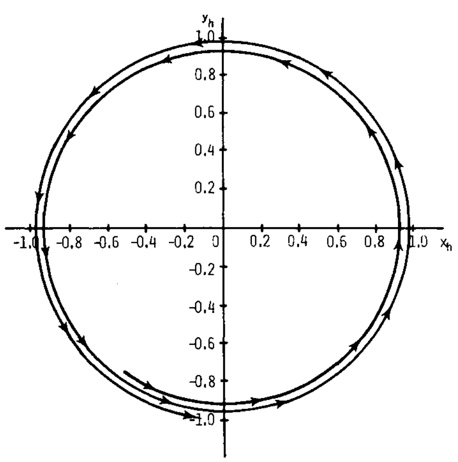


**Fig. 9 Projection of the terminus of $\hat{\mathbf{k}}$ into the $x_h y_h$-plane.**

a spacecraft to scan a portion of the celestial sphere and then be returned to an inertial orientation.

Finally, it is *theoretically* possible to produce an almost complete ($k\simeq 1$, $\gamma_m \simeq 180°$) rotation of an axis of a spinning spacecraft which would have a definite period, ninety minutes, one day, etc. Whether this is *practically* possible remains to be seen. If the tumbling time is to be very long compared to $2\pi/\Omega$, $K$ must be made very large and/or $\lambda$ must be made very small. As mentioned previously, making $K>6$ would be difficult. To make $\lambda$ small, $B$ and $C$ could be made very nearly equal. The accuracy with which this may be done should be studied.

## Conclusion

The effects of mass redistribution on the rotational motion of an initially uniformly spinning, free body have been studies using a simple three-body model. An exact analytical solution for the motion of the original spin axis of the system after mass redistribution has been developed using the classical solution for the rotational motion of a free, triaxial, rigid body and a geometrical interpretation of the analytical results has been presented.

By proper choice of the system parameters and the motion of the control masses it has been shown that various motions of the original spin axis may be obtained. Examples of such motions were discussed. These results support previous contentions[3,4] that mass redistribution may be used to "control" the attitude of an artificial satellite "semipassively."

If the time of mass redistribution is small compared with the polhodic period of the resulting rigid body motion, it is permissible, in a first approximation, to neglect the dynamic effects of the control mass motion and use the analytical results given here to predict the motion of the system's original spin axis. Furthermore, if the control masses are moved to the desired final locations in a carefully chosen manner, the dynamic effects of control mass motion may be predicted very accurately by approximate solutions of the equations of motion of the "changing" system.

## Appendix

The results stated in Eqs. (3) and (4) may be obtained by considering Euler's equations,

$$\begin{aligned} A\dot{\omega}_{x'} + (C-B)\omega_{y'}\omega_{z'} &= 0 \\ B\dot{\omega}_{y'} + (A-C)\omega_{x'}\omega_{z'} &= 0 \\ C\dot{\omega}_{z'} + (B-A)\omega_{y'}\omega_{x'} &= 0 \end{aligned} \tag{A1}$$

and the kinematic equations,

$$\begin{aligned} \omega_{x'} &= \dot{\phi} - \dot{\psi}\sin\theta \\ \omega_{y'} &= \dot{\psi}\cos\theta\,\sin\phi + \dot{\theta}\cos\phi \\ \omega_{z'} &= \dot{\psi}\cos\theta\,\cos\phi - \dot{\theta}\sin\phi \end{aligned} \tag{A2}$$

$$\mathbf{h} = h(-\sin\theta\hat{\mathbf{i}}' + \cos\theta\,\sin\phi\hat{\mathbf{j}}' + \cos\phi\,\cos\phi\hat{\mathbf{k}}')$$

$$\mathbf{h} = A\omega_{x'}\hat{\mathbf{i}}' + B\omega_{y'}\hat{\mathbf{j}}' + C\omega_{z'}\hat{\mathbf{k}}' \tag{A3}$$

where $\hat{\mathbf{i}}'$, $\hat{\mathbf{j}}'$, and $\hat{\mathbf{k}}'$ are unit vectors associated with the $Cx'y'z'$ system.

The two integrals,

$$A\omega_{x'}^2 + B\omega_{y'}^2 + C\omega_{z'}^2 = 2T = \text{constant} \tag{A4}$$

and

$$A^2\omega_{x'}^2 + B^2\omega_{y'}^2 + C^2\omega_{z'}^2 = h^2 = \text{constant} \tag{A5}$$

of Eqs. (A1) may be used in the second of Eqs. (A1) to obtain

$$\dot{\omega}_{y'}^2 = (a - b\omega_{y'}^2)(d - e\omega_{y'}^2)/(AB^2C) \tag{A6}$$

where $a=h^2-2AT$, $b=B(B-A)$, $d=2CT-h^2$ and $e=B(C-B)$. Then letting $\omega_{y'}=Q\sin\xi$, where $Q$ is to be chosen in what follows and $\xi$ is a new variable, we get

$$\dot{\xi}^2 = (a - bQ^2\sin^2\xi)(d - eQ^2\cos^2\xi) \div AB^2CQ^2\cos^2\xi \tag{A7}$$

Setting $Q^2 = d/e$, we obtain

$$\dot{\xi}^2 = \lambda^2(1 - k^2\sin^2\xi) \tag{A8}$$

where

$$\lambda^2 = [(C-B)(h^2-2AT)]/ABC \tag{A9}$$

and

$$k^2 = [(B-A)(2CT-h^2)]/[(C-B)(h^2-2AT)] \tag{A10}$$

It follows from Eq. (A8) that $\sin\xi = \mathrm{snu}$ and hence

$$\omega_{y'} = Q\, sn\, u \tag{A11}$$

where $u = \lambda t - \nu$ and $\nu$ is a constant of integration. For $C > B > A$, the integrals (A4) and (A5) and Eq. (A11) may be used in conjunction with Eqs. (A1) to obtain

$$\omega_{x'} = P\, cn\, u \tag{A12}$$

and

$$\omega_{z'} = R\, dn\, u \tag{A13}$$

where $P = \{(2CT - h^2)/[A(C-A)]\}^{1/2}$

and $R = \{(h^2 - 2AT)/[C(C-A)]\}^{1/2}$

Letting $p = AP/h$, $q = BQ/h$ and $r = CR/h$, we have, from Eqs. (A3), (A11), (A12) and (A13),

$$\begin{aligned} -\sin\theta &= p\, cnu \\ \cos\theta\, \sin\phi &= q\, sn\, u \\ \cos\theta\, \cos\phi &= r\, dn\, u \end{aligned} \tag{A14}$$

From Eqs. (A2), we obtain

$$\dot{\psi} = (h/C)[1 + [(C-B)/B]\sin^2\phi] \tag{A15}$$

Then, by using $\tan\phi = (B/C)(Q/R)(\mathrm{snu}/\mathrm{dnu})$, we find that

$$\psi = \psi_1 + \int_{t_1}^{t} (h/C)[1 + g^2(\frac{sn^2 u}{1 + \sigma^2 sn^2 u})]dt \tag{A16}$$

where

$$g^2 = \sigma^2 (C-A)/A$$

$$\sigma^2 = [A(C-B)]/[C(B-A)]k^2 \tag{A17}$$

The integral in Eq. (A16) may be evaluated in terms of Jacobi's Theta and Zeta functions.[8] The result is ($\sigma^2 \neq 0, -1, \infty$ or $-k^2$)

$$\psi = \psi_1 + n(t - t_1) - \frac{i}{2} ln[\frac{\Theta(u - ia')\Theta(\nu - ia')}{\Theta(u + ia')\Theta(\nu + ia')}] \tag{A18}$$

where

$$n = (h/C) i Z(ia')\lambda$$

$$i = \sqrt{-1}$$

$$a' = -i\, sn^{1}(\sigma/ik) \tag{A19}$$

$\Theta(\ )$ = Jacobi's Theta function

$Z(\ )$ = Jacobi's Zeta function

Equations (A14) are not in forms well suited to the introduction of arbitrary initial values, say $\omega_{x'}(0)$, $\omega_{y'}(0)$, and $\omega_{z'}(0)$, of the angular velocity components. To obtain more useful equations, we use the identities (Ref. 7, p. 23),

$$\begin{aligned} sn\, u \equiv sn(\lambda t - \nu) &\equiv [sn\lambda t\, cn\nu\, dn\, \nu - sn\, \nu\, cn\, \lambda t\, dn\, \lambda t]/\Delta \\ cn\, u \equiv cn(\lambda t - \nu) &\equiv [cn\, \lambda t\, cn\, \nu + sn\, \nu\, dn\, \nu\, \lambda t\, dn\, \lambda t]/\Delta \\ dn\, u \equiv dn(\lambda t - \nu) &\equiv [dn\, \lambda t\, dn\, \nu + k^2 sn\, \nu\, cn\, \nu\, sn\lambda t\, cn\lambda t]/\Delta \end{aligned} \tag{A20}$$

where $\Delta = 1\text{-}k^2 sn^2 \lambda t\, sn^2 \nu$.

When $t = 0$, from Eqs. (A11-A14), we have

$$\begin{aligned} sn\, \nu &= -\omega_{y'}(0)B/qh \\ cn\, \nu &= \omega_{x'}(0)A/ph \\ dn\, \nu &= \omega_{z'}(0)C/rh \end{aligned} \tag{A21}$$

Since $\lambda$, $k$, $h$, $p$, $q$, and $r$ are defined in terms of the initial values of the components of angular velocity, Eqs. (A21) when inserted into Eqs. (A20) yield the required expressions for the elliptic functions.

## References


[1] MacMillan, W. D., *Dynamics of Rigid Bodies*, Dover, New York, 1960, pp. 208-211.

[2] Beachley, N. H. and Uicker, J. J., Jr., "Reply by Authors to L. H. Grashoff," *Journal of Spacecraft and Rockets,* Vol. 6, Oct. 1969, pp. 1215-1216.

[3] Beachley, N. H., "Inversion of Spin-Stabilized Spacecraft by Mass Translation—Some Practical Aspects," *Journal of Spacecraft and Rockets,* Vol. 8, Oct. 1971, pp. 1078-1080.

[4] Kane, T. R. and Scher, M. P., "A Method of Active Attitude Control Based on Energy Considerations," *Journal of Spacecraft and Rockets,* Vol. 6, May 1969, pp. 633-636.

[5] Lorell, K. R. and Lange, B. O., "An Automatic Mass-Trim System for Spinning Spacecraft," *AIAA Journal,* Vol. 10, Aug. 1972, pp. 1012-1015.

[6] Whittaker, E. T., *Analytical Dynamics of Particles and Rigid Bodies,* Cambridge University Press, New York, 1944, pp. 144-152.

[7] Byrd, P. F. and Friedman, M. D., *Handbook of Elliptic Integrals for Engineers and Scientists,* Springer-Verlag, Berlin, Germany, 1971, pp. 17, 323-330.

[8] Whittaker, E. T. and Watson, G. N., *Modern Analysis,* Cambridge University Press, Cambridge, England, 1963, pp. 522-523.